The interpretation of spin-polarized photoemission spectra by the spin-spiral model: application to measurements on Ni(111)

1994 J. Phys.: Condens. Matter 6 3609

(http://iopscience.iop.org/0953-8984/6/19/017)

J. Phys.: Condens. Matter 6 (1994) 3609–3617. Printed in the UK

The interpretation of spin-polarized photoemission spectra by the spin-spiral model: application to measurements on Ni(111)

Alfred Ziegler† and Rainer Böttner‡

† Institut für Theoretische Physik der Universität Frankfurt, Robert-Mayer-Strasse 8, D-60054 Frankfurt, Germany

‡ Physikalisches Institut der Universität Frankfurt, Robert-Mayer-Strasse 2–4, D-60054 Frankfurt, Germany

Received 1 September 1993, in final form 20 January 1994

Abstract. A generalization of the spin-spiral model developed previously to interpret non-spin-polarized photoemission data on ferromagnetic metals to the spin-polarized case is applied to measurements on nickel by Kämper *et al*. This method is easy to use and in contrast to the cumbersome random-cluster model leads to meaningful results for the magnetic short-range order ranging from 20 Å to 60 Å close to T_c.

1. Introduction

One of the still unresolved problems in the theory of ferromagnetic metals is the characterization of the magnetic excitations at finite temperatures. This includes the well known problems of calculating the Curie temperature and of determining the amount of short-range-order above it. Because the interpretation of neutron-scattering data has been subject to controversy [1–12] angle-resolved ultraviolet photoemission spectroscopy has served as a prominent tool in investigating this problem. Due to the indirect nature of this probe—it basically determines the one-electron states established by scattering off the magnetic excitations—a fair amount of theoretical interpretation is necessary in order to draw conclusions from measured spectra. Particularly well known are the works of Korenman and Prange [20, 21, 14], Usami and Moriya [16] and Staunton *et al* [19]. Unfortunately they apply only to the limiting cases of massive and vanishing short-range-order. Therefore attempts were made to find models valid for the continuous range of possible short-range-order, viz. the spin-spiral model [22, 24] and the random-cluster approach [22, 23]. The random-cluster approach is accurate but numerically cumbersome and does not lead to an analytic lineshape that might be used in fitting procedures (as is usually done in interpreting spectra) whereas the spin-spiral model is physically transparent and leads to analytic lineshapes but is overly simplistic. Initially photoemission spectroscopy was done above T_c and without spin analysis [14, 26, 27, 28], but the unpolarized data did not resolve all issues, particularly in the case of nickel, so a number of spin-polarized measurements (below T_c of course) were undertaken [18, 17, 13].

The aim of this article is to generalize the spin-spiral model, which in its original form is unsuitable for the polarized case, to spin-polarized measurements and to demonstrate how simple its application is by using it to interpret the experiments on Ni(111) by Kämper *et al*

0953-8984/94/193609+09$19.50

[13], which are particularly suitable for this purpose because they have also been interpreted by the random-cluster technique [23].

In section 2 the method is presented with sufficient detail that prospective users can put it to immediate use. Section 3 describes the application to the nickel experiments, i.e. the detailed fit and the discussion of the results.

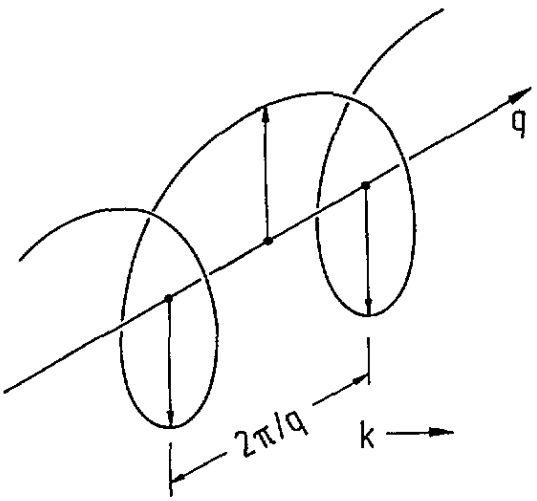

Figure 1. An electron wavefunction, where the direction of the electron spin varies when one progresses in physical space in a direction called the 'spiral axis' by turning uniformly in a plane perpendicular to the spiral axis, is called a spin spiral. The period of the turn is given by $2\pi/q$ where q is the 'wavevector' of the spiral.

2. A description of the model

In the spin-spiral approach [22] the magnetic structure is modelled as a kind of generalized mean field: there is an effective magnetic field leading to an exchange splitting Δ in the ground state, which has constant magnitude but varies in direction in the following way (figure 1): by moving along a given direction in the crystal (termed the spiral axis) the direction of the field rotates by an angle $\varphi = qr$ in the plane *perpendicular* to the spiral axis, where r is the distance travelled and q characterizes the amount of torsion, i.e. how fast the direction of the magnetic field turns. Because translation invariance is broken the momentum $\hbar k$ is no longer a good quantum number. What is seen in photoemission is the projection of the eigenfunctions onto the Bloch states obtained for $\Delta = 0$. The spectral function for given momentum k that results from this projection has four peaks per paramagnetic band ε_k (that obtained for $\Delta = 0$) at the energies

$$E = \varepsilon_k + \frac{\varepsilon_{k\pm q} + \varepsilon_k}{2} \pm \frac{1}{2}\sqrt{(\varepsilon_{k\pm q} - \varepsilon_k)^2 + \Delta^2} \tag{1}$$

with weights

$$w = \left(1 + \left(\frac{E - \varepsilon_k}{\Delta/2}\right)^2\right)^{-1}$$

(figure 2, see [22] for details). Figure 3 shows lineshapes for a simple tight-binding band $\varepsilon_k = w \cos k$ for $w/\Delta = 1$, $k = 0$ and $\pi/2$ and various values of q, where some Lorentzian

broadening has been added to simulate the effects of unavoidable experimental (and many-body) broadening. Although there are four peaks in general they are symmetric for $k = \pi/2$ and twofold degenerate for $k = 0$. For $k = \pi/2$ the two ferromagnetic peaks separated by Δ split into two peaks each, which move apart with increasing disorder (increasing q), with the outward-moving peaks rapidly losing weight and the approaching peaks becoming more intense, leading to a lineshape where one sees two ferromagnetic peaks that broaden, then move together and merge to a central peak that becomes increasingly narrower. In the $k = 0$ case, in contrast, there are two peaks only: one moving inward with its weight increasing, the other one moving outward and dying out, so in the lineshape one sees two peaks at first with one of them becoming imperceptible after a while. No narrowing of the remaining line is to be expected.

In order to calculate spin-resolved spectra we start by decomposing the eigenfunction of a spiral configuration into its spin components parallel or antiparallel *relative to the local direction of magnetization defined by the spiral.* Contrary to what one may expect the electrons scattered by the spin spiral by no means have their spins aligned with the potential. They have a form of 'spin inertia,' which keeps them from fully following the turn of the magnetization direction: in moving from one site to the next they respond to the change in magnetization, which exerts a torque, by precessing around the new direction. The larger the tilt q is, the larger is the opening angle θ of the precession cone (figure 4). For an electron with a definite spin state in a direction on the cone the respective probabilities for measuring up or down spin with reference to the direction of the magnetizing field perpendicular to the spiral axis are

$$p_\uparrow = \cos^2(\pi/2 - \theta)/2 = (1 + \sin\theta)/2 \tag{2a}$$

$$p_\downarrow = \sin^2(\pi/2 - \theta)/2 = (1 - \sin\theta)/2 \tag{2b}$$

or

$$p_\sigma = (1 + \sigma \sin\theta)/2 = (1 + 2\sigma \sin(\theta/2)\cos(\theta/2))/2. \tag{2c}$$

Note that one cannot use plain trigonometry here because there are only two states to project to; rather one has to take—as is familiar in the spin case—*half* the angles expected from naive trigonometry.

This spin decomposition in the local frame of reference (where 'up' is always in the direction of the spiral magnetization) now has to be related to the decomposition in the laboratory frame of reference. The basic picture used for that purpose is derived from local-band theory [29, 30], where it is assumed that there is enough magnetic short-range order to define domains with more or less homogeneous magnetization large enough to have a band structure. These domains then act thermodynamically like macrospins in an effective Heisenberg Hamiltonian. The model we use here is somewhat different insofar as we do not take the magnetization in a domain to be absolutely homogeneous but somewhat disordered, i.e. it can be described by sections of spin spirals or incomplete spirals (a spiral of infinite length has magnetization zero).

In setting up the lineshape in the laboratory system one consequently has to use

$$L_\sigma^{\text{lab}}(E) = (1 + \sigma m(T))L_\sigma(E) + (1 - \sigma m(T))L_{-\sigma}(E) \tag{3}$$

because if $L_\sigma(E)$ denotes the lineshape of a domain with its macrospin pointing in the direction of the net magnetization one finds domains with spins parallel to the net magnetization with probability $1+\sigma m(T)$ and those antiparallel with probability $1-\sigma m(T)$, where $m(T) = M(T)/M(0)$ is the relative magnetization. $L_\sigma(E)$ of course has to include the precession effect mentioned above because the field within the domain is *not* homogeneous but spiral like. Equation (2) cannot be used directly, however, because the

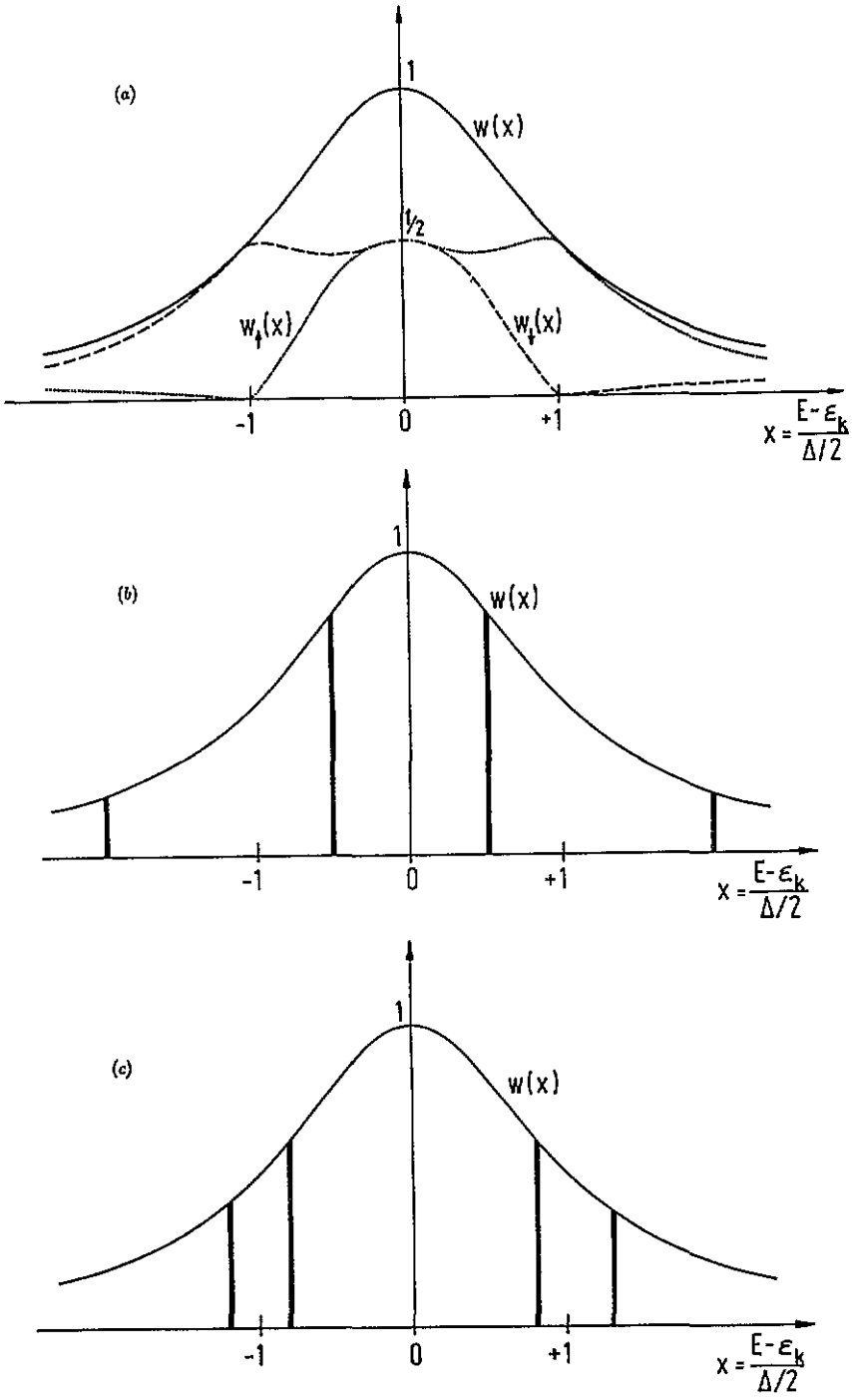

Figure 2. (*a*) Irrespective of how large the disorder parameter q is the weights w_i and $w_{i\sigma}$ (for the unpolarized and polarized cases respectively) do not depend on q directly but only on the energy $x = (E - \varepsilon_k)/(\Delta/2)$. (*b*) Spectral lines (without experimental broadening) for $k = \pi/2$ and weak disorder q. (*c*) As (*b*) but with strong disorder q.

projection onto a definite wavevector k already leads to different weights for opposite spins

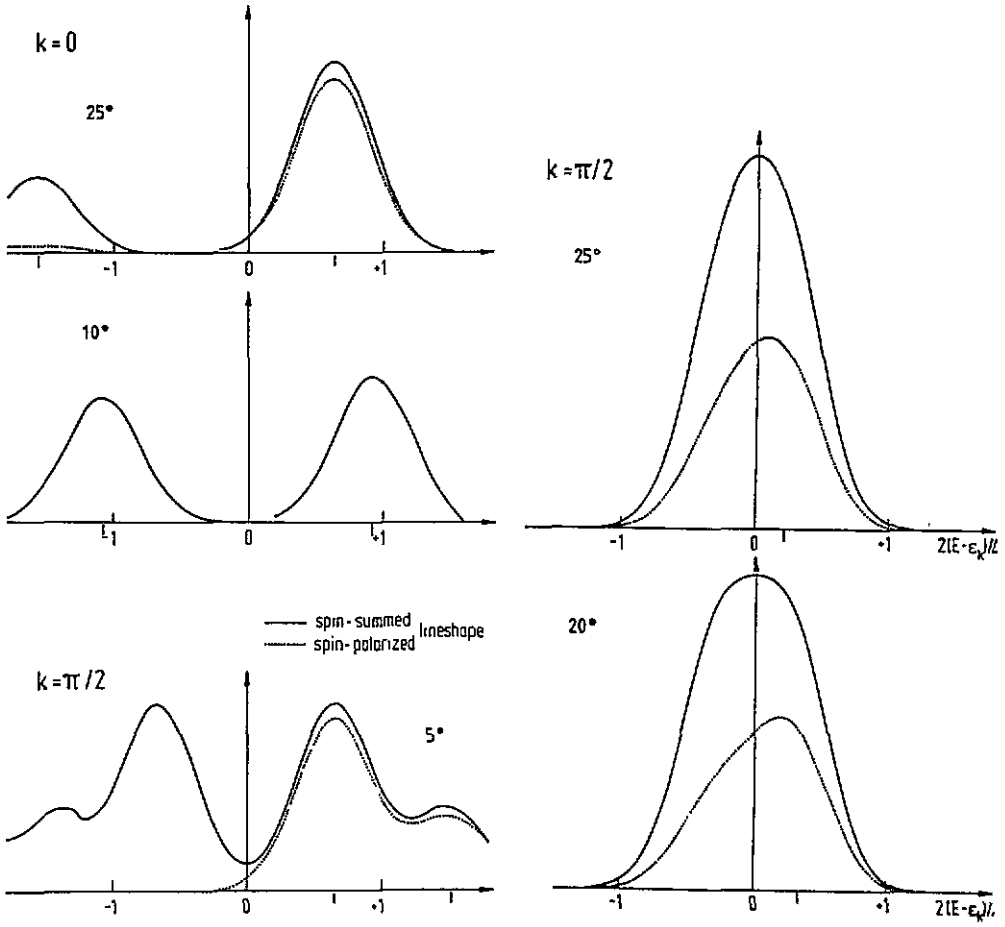

Figure 3. Spin-summed (full curves) and majority-spin (dotted curves) photoemission lineshapes for various turn angles of the magnetization from one lattice site to its nearest neighbour for $k = 0$ and $k = \pi/2$ including experimental broadening.

in the following way: the (spin-summed) weights of the electron states given above are related to the angle θ the cone forms with the spiral axis by $w = \cos^2 \theta/2$ where θ is given by

$$\tan \theta/2 = (E - \varepsilon_k)/(\Delta/2)$$

(see [22]). The four energies in the lineshape fall into two pairs, where each pair consists of electron states with angles $\theta = \tilde{\theta}$ and $\theta = \pi - \tilde{\theta}$, i.e. exactly opposite spins, and whose energies consequently lie on *opposite* sides of the $(E - \varepsilon_k)/(\Delta/2)$-axis. This leads to

$$L_\sigma(E) = N^{-1}(w(E_1)p_\sigma(\tilde{\theta})\delta(E - E_1) + w(E_2)p_{-\sigma}(\tilde{\theta})\delta(E - E_2)) \qquad (4)$$

where

$$w(E_1) = \cos^2 \tilde{\theta}/2$$
$$w(E_2) = \sin^2 \tilde{\theta}/2$$

where use has been made of the relation

$$p_\sigma(\pi - \tilde{\theta}) = p_{-\sigma}(\tilde{\theta}).$$

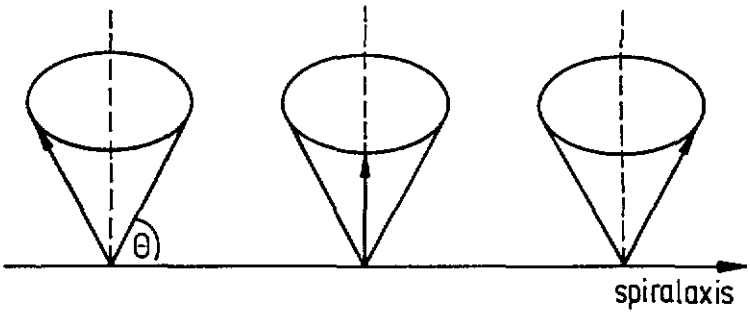

Figure 4. The spin vectors of electrons scattered by a spin spiral do not point in the direction of the spiral but form a precession cone with opening angle $\pi/2 - \theta$. The figure shows the precession cone in a system of reference where the twist of the spiral has been undone, i.e. where the spiral acts like a homogeneous field.

The normalization factor

$$N = w(E_1)p_\sigma + w(E_2)p_{-\sigma} = (1 + \tfrac{1}{2}\sin 2\tilde{\theta})/2 \tag{5}$$

was introduced to guarantee that the total weight w_σ of $L_\sigma(E)$ is equal to $\frac{1}{2}$.

This expression is somewhat cumbersome for numerical handling and may be substituted for without much loss in accuracy by replacing

$$w_{i\sigma} = \frac{w_i}{2}(1 \pm 2\sigma\sqrt{w_i(1-w_i)}) \tag{6}$$

with

$$w_{i\sigma} = \frac{w_i}{2}(1 \pm \sigma\, 4(1-w_i)^2) \qquad \text{for } w_i > \tfrac{1}{2}$$

$$w_{i\sigma} = \frac{w_i}{2}(1 \pm \sigma\, 4w_i(1-w_i)) \qquad \text{for } w_i < \tfrac{1}{2}$$

where the positive sign is valid for positive values and the negative sign for negative values of $(E - \varepsilon_k)/(\Delta/2)$. This weight function is plotted in figure 2. The spin-resolved lineshapes are given in figure 3 (note that these curves function is plotted in figure 2. The spin-resolved lineshapes are given in figure 3 (note that these curves include the depolarization part only, not the weighting by $1 + \sigma m(T)$). One sees that a line moving inward basically keeps its weight with respect to the opposite spin direction. Thus for $k = 0$ where there is relatively little movement there is a tendency for two pure peaks in the spin-resolved spectra whereas for $k = \pi/2$ with its rapidly moving lines the spin-resolved spectra contain peaks that have a secondary maximum. For comparison with experiment one has to include the weighting by $1 + \sigma m(T)$ as well, leading to equation (3). An example is given in the next section.

3. Application to spin-resolved spectra from Ni(111)

In this section the method introduced in the previous section is applied to measurements by Kämper *et al* [13] on nickel along the Λ-line in the Brillouin zone (see figure 5). They took spin-polarized spectra at three different points for a range of temperatures between room temperature and T_c. These experiments were inspired by corresponding measurements in iron [18, 28] that had shown that the spectra may behave quite differently as a function of temperature at different points in the Brillouin zone. Earlier measurements in nickel had concentrated on the S-line in the vicinity of the X-point, so it was desirable to look

at a different part of the Brillouin zone to see whether there is a similar variation in the temperature-dependent spectra. In contrast to the X measurements non-spin-resolved spectra are not very meaningful because of the significantly larger broadening. Although Kämper *et al* found quite some variation even among the three points along the Λ-line, they found it difficult to interpret the spectra in terms of the amount of short-range order present. Gollisch and Feder [23], using the random-cluster model, were able to reproduce the spectra but because of the large broadening their lineshapes are quite insensitive to the amount of short-range order used in the calculation, so no conclusions could be drawn.

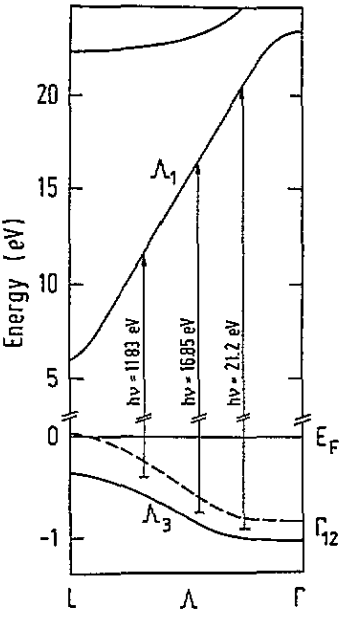

Figure 5. The band structure of Ni along the Γ–L-line indicating the points of measurement (from [13]).

In our approach the lineshapes were fitted by an equation of the form

$$I_\sigma(E) = I_{BG} + S_\sigma(e^{\beta(E-E_F)})^{-1} \sum_{i=1,\sigma}^{4} w_{i\sigma}(1+\sigma m(T))\frac{1}{\pi}\frac{\gamma_i}{(E-E_i)^2+\gamma_i^2}$$

where I_{BG} is the background intensity, S_σ a spin-dependent scaling factor and $m(T)$ the relative magnetization. E_i are the four energies per band given above, $w_{i\sigma}$ the corresponding weights and γ_i a damping factor. It is important to note that the w_σ and E_i are *not* independent fitting factors but are determined by the single parameter q, where the ε_k used in the expression for the E_i was fitted to the actual band in figure 5. A typical fit is shown in figure 6.

In contrast to [23] it is possible by our method to derive meaningful values for the short-range-order parameter q (figure 7). As can be seen the disorder increases with temperature, but it is not obvious whether or at what value it saturates. More interestingly the disorder in this interpretation is *not* the same for the three points in the Brillouin zone, as one expects it to be, larger values being obtained the closer one is to the L-point. The reason for this behaviour is not clear, although it should be mentioned that it has also been seen in the spin-spiral interpretation of non-spin-resolved spectra taken at different points along the S-line [26].

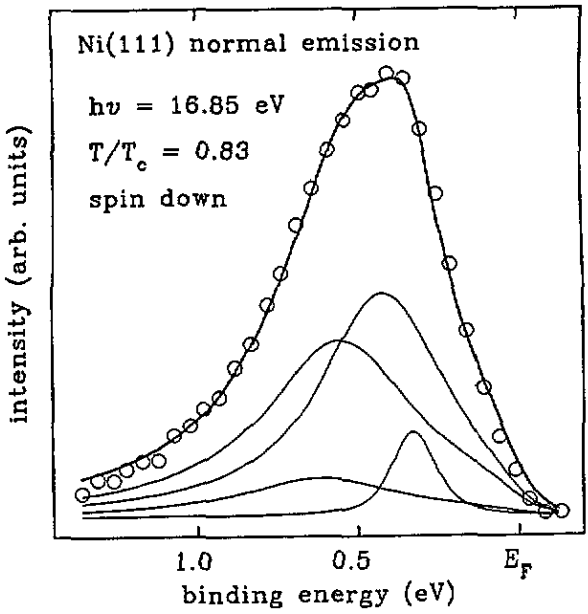

Figure 6. An example of a fitted lineshape: the circles are the measured data, the lines are obtained by the fit.

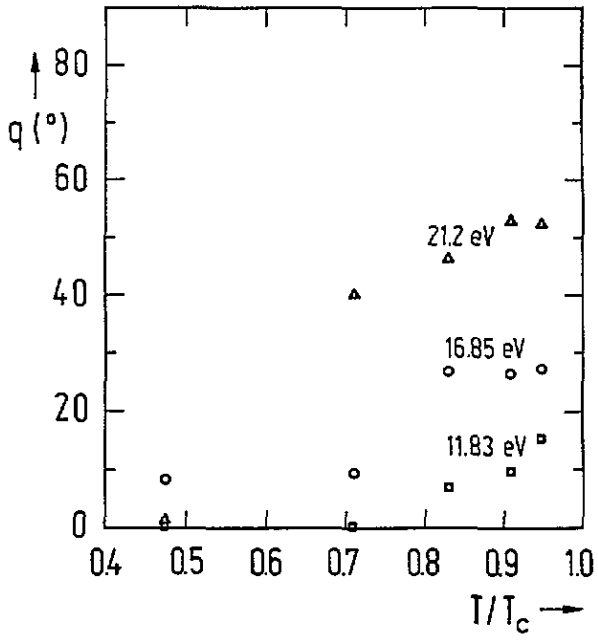

Figure 7. The tilt parameter $q = \lambda^{-1}$, where λ is a length characterizing the magnetic short-range order, plotted as a function of temperature for the three points in the Brillouin zone given in figure 5. Triangles denote the 21.2 eV measurements, circles and squares those for 16.85 eV and 11.83 eV respectively.

In conclusion we have shown that the spin-spiral method for interpreting photoemission

spectra can be generalized to the spin-polarized case and also by applying it to a concrete experiment, that it is both easier to handle and leads to more definite results than the random-cluster model.

Acknowledgments

We gratefully acknowledge the cooperation of K P Kämper and G Güntherodt from TH Aachen, who provided the experimental data for analysis.

A preliminary report of the method has appeared in [3].

References

[1] Brown P J, Capellmann H, Dèportes J, Givord D and Ziebeck K R A 1982 *J. Magn. Magn. Mater.* **30** 243
[2] Edwards D M 1983 *J. Magn. Magn. Mater.* **36** 213
[3] Ziegler A 1992 *J. Magn. Magn. Mater.* **101–103** 671
[4] Wicksted J P, Shirane G and Steinsvoll O 1984 *Phys. Rev.* B **29** 488
[5] Brown P J, Capellmann H, Dèportes J, Givord D, Johnson S M, Lynn J W and Ziebeck K R A 1985 *J.Physique* **46** 827
[6] Lynn J W 1975 *Phys. Rev.* B **11** 2624
Mook H A, Lynn J W, Nicklow R M 1973 *Phys. Rev. Lett.* **30** 556
Lynn J W and Mook H A 1981 *Phys. Rev.* B **23** 198
[7] Mook H A 1981 *Phys. Rev. Lett.* **46** 508
[8] Steinsvoll O, Majkrzak C F, Shirane G and Wicksted J 1983 *Phys. Rev. Lett.* **51** 300
Uemura Y J, Shirane G, Steinsvoll O and Wicksted J 1983 *Phys. Rev. Lett.* **51** 2322
Wicksted J, Shirane G and Steinsvoll O 1984 *Phys. Rev.* B **29** 488
Steinsvoll O, Majkrzak C F, Shirane G and Wicksted J 1984 *Phys. Rev.* B **30** 2377
[9] Wicksted J, Shirane G and Steinsvoll O BNL-33849 (unpublished)
[10] Böni P and Shirane G 1985 *J. Appl. Phys.* **57** 3012
[11] Mook H A and Lynn J W 1985 *J. Appl. Phys.* **57** 3006
[12] Martinez J L, Böni P and Shirane G 1985 *Phys. Rev.* B **32** 7037
Shirane G, Böni P and Martinez J L 1987 *Phys. Rev.* B **36** 881
[13] Kämper K P, Schmitt W and Güntherodt G 1990 *Phys. Rev.* B **42** 10 696
[14] Dietz E, Gerhardt U and Maetz C J 1978 *Phys. Rev. Lett.* **40** 892
Maetz C J, Gerhardt U, Dietz E, Ziegler A and Jelitto R J 1982 *Phys. Rev. Lett.* **48** 1686
[15] Raue R, Hopster H and Clauberg R 1984 Z. *Phys.* B **54** 121
[16] Usami K and Moriya T 1980 *Solid State Commun.* **36** 619
[17] Hopster H, Raue R, Güntherodt G, Kisker E, Clauberg R and Campagna M 1983 *Phys. Rev. Lett.* **51** 829
[18] Kisker E, Schröder K, Campagna M and Gudat W 1984 *Phys. Rev. Lett.* **52** 2285
Kisker E, Schröder K, Gudat W and Campagna M 1985 *Phys. Rev.* B **31** 329
[19] Staunton J, Gyorffy B L, Pindor A J, Stocks G M and Winter H 1985 *J. Phys. F: Met. Phys.* **15** 1387
[20] Korenman V and Prange R E 1980 *Phys. Rev. Lett.* **44** 1291
[21] Korenman V and Prange R E 1984 *Phys. Rev. Lett.* **53** 186
[22] Haines E M, Heine V and Ziegler A 1985 *J. Phys. F: Met. Phys.* **15** 661; 1986 *J. Phys. F: Met. Phys.* **16** 1343
[23] Gollisch H and Feder R 1990 *Solid State Commun.* **76** 237
[24] Ziegler A 1983 *J. Magn. Magn. Mater.* **31–34** 297
[25] Mohn P and Wohlfarth E P 1987 *J. Phys. F: Met. Phys.* **17** 2421
Mohn P, Wagner D and Wohlfarth E P 1987 *J. Phys. F: Met. Phys.* **17** L13
Wohlfarth E P and Mohn P 1988 *Physica* B **149** 145
Wagner D and Wohlfarth E P 1986 *Phys. Lett.* **A118** 29
[26] Würtenberg J 1987 *Thesis* University of Frankfurt
[27] Eastman D E, Himpsel F J and Knapp J A 1978 *Phys. Rev. Lett.* **40** 1514
[28] Kirschner J, Glöbl M, Dose V and Scheidt H 1984 *Phys. Rev. Lett.* **53** 612
[29] Korenman V, Murray J and Prange R E 1977 *Phys. Rev.* B **16** 4032, 4048, 4058
[30] Ziegler A 1982 *Phys. Rev. Lett.* **48** 695